MIT Libraries | DSpace@MIT

MIT Open Access Articles

The Anatomy of Knock

Massachusetts Institute of Technology

The Anatomy of Knock

Author, co-author (Do NOT enter this information. It will be pulled from participant tab in MyTechZone)

Affiliation (Do NOT enter this information. It will be pulled from participant tab in MyTechZone)

Abstract

The combustion process after auto-ignition is investigated. Depending on the non-uniformity of the end gas, auto-ignition could initiate a flame, produce pressure waves that excite the engine structure (acoustic knock), or result in detonation (normal or developing). For the "acoustic knock" mode, a knock intensity (KI) is defined as the pressure oscillation amplitude. The KI values over different cycles under a fixed operating condition are observed to have a log-normal distribution. When the operating condition is changed (over different values of λ, EGR, and spark timing), the mean (μ) of log (KI/GIMEP) decreases linearly with the correlation-based ignition delay calculated using the knock-point end gas condition of the mean cycle. The standard deviation σ of log(KI/GIMEP) is approximately a constant, at 0.63. The values of μ and σ thus allow a statistical description of knock from the deterministic calculation of the ignition delay using the mean cycle properties

Introduction

Reducing the engine displacement while maintaining the engine torque output by boosting is an effective strategy to improve the fuel economy of SI engines. Such engines work at very high mean effective pressure and engine knocking is an important limiting factor. There is a large body of literature on engine knock [1]. Knock research has focused on two aspects: the phenomena leading to knock, and what happens when knock occurs. The former category, which constitutes the major part of the literature, includes the study of ignition delay through measurements in shock tubes and rapid compression machines [2, 3], modeling by basic chemical kinetics [4, 5], developing empirical correlations via engine data [6, 7], and assessing the fuel effects [8, 9]. The Livengood and Wu integral [10] is used to relate the fuel air mixture ignition delay behavior to the knock on set in an engine. The latter category includes the visualization of the knock phenomenon [11, 12], and the numerical simulation of knock in a fuel air mixture [13].

This paper addresses the combustion phenomena after the onset of knock. The different combustion modes are discussed first. Then for the "acoustic knock" mode, which is the one most encountered in engine calibration, the statistics of the amplitude of the pressure oscillation is assessed.

Modes of Knock Combustion

Knock is the auto-ignition of the unburned mixture. In most cases, the compression of the end gas in a SI engine would increase the end gas temperature and density, thereby accelerate the chemistry and lead to auto-ignition. The end gas is non-uniform in temperature and composition. Because of this non-uniformity, three modes of post-knock combustion have been identified [13]

(i)   Deflagration
(ii) Thermal explosion
(iii) Developing detonation

When a mass of air/fuel mixture is auto-ignited, the local pressure build up is the result of the competition between the heat release rate and the pressure relief due to the volumetric expansion of the burned mixture; see Fig. 1. For illustration purpose, assume that the burned gas is perfect (ideal gas with constant properties), the 1st law of thermodynamics applied to the auto-ignition region becomes:

$$\frac{dp}{dt} = (\gamma - 1)\dot{q} - \gamma p \frac{\dot{V}}{V} \qquad (1)$$
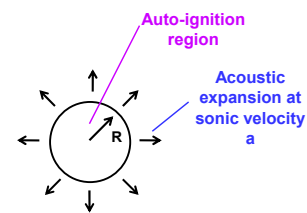

Figure 1. Illustration of pressure build up in knock combustion.

Here P is the pressure, $\dot{q}$ is the heat release rate per unit volume, and V is the volume of the auto-ignited region. (See definitions/ abbreviations section at the end of the paper for explanation of the symbols.) Thus local pressure will build up if the heat release term is large compare to the volumetric expansion term [14, 15]:

$$\dot{q} >> \frac{\gamma}{\gamma - 1} p \frac{\dot{V}}{V} \qquad (2)$$

The expansion rate for the ignited region is at the acoustic velocity a. For a spherical auto-ignition region of radius R, the criterion of Eq.(2) becomes

7/20/2015

$$\dot{q} >> \frac{\gamma}{\gamma - 1} p \frac{3a}{R}$$

<div align="right">(3)</div>

Note the dependence of the criterion on the size R of the ignited region (exothermic center) in relationship to the volumetric heat release rate $\dot{q}$. When R is small, the acoustic expansion can easily relax the pressure build up due to heat release.

The consequence of the three modes are described in the following.

(a) flame initiation

When R is small, there is very little pressure build up; hence there will be no or very weak acoustic wave developed. The small R is associated with steep gradients (temperature and/or composition) in the non-uniform end gas, thereby the regions of ignition are small islands at, for example, maximum local temperature. The radicals and high local temperature of the ignited region initiates a flame (a deflagration, or subsonic propagation of the heat release front) in the unburned mixture. A good example of that is in the sporadic pre-ignition (SPI) event in highly loaded engines [16]. Fig. 2 shows pressure traces of such engine. For the SPI pressure trace, ignition of oil vapor or other sources comprises a small auto-ignited region which initiates a flame. However, the pressure trace after ignition (at -19° atdc) does not exhibit any pressure oscillation until the end gas auto-ignites.
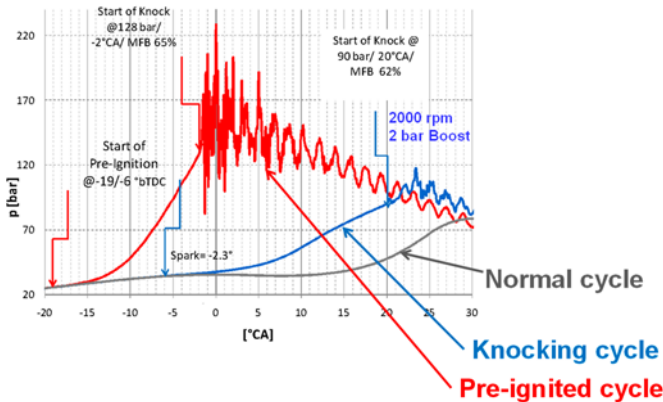

Figure 2. Pressure from sporadic pre-ignition event.

(b) Acoustic knock

When R is moderately large so that the criterion of Eq. (3) is satisfy, there is significant local pressure build up and pressure waves (acoustic waves) or even weak shock waves are excited. This mode is termed "thermal explosion" in Ref. [13] because there is fast heat release from a sizable region. These waves could be of minor annoyance to the driver, or be quite intense and cause damage to the engine via the repeated pounding on the combustion chamber surfaces by the local high pressure and high temperature. However, these pressure waves are not strong enough to initiate Chapman-Jouguet type of denotation [17]. The major manifestation of the pressure wave is the excitation of the engine structural vibration; hence the phenomenon is term acoustic knock.

Depending on the temperature/ composition non-uniformity in the end gas, there could be sequential auto-ignition of isolated regions, or successive-ignition of connected regions - for example, along a

temperature gradient [13, 17, 18]. In the former, a flame is initiated at the outer boundary of the auto-ignited region. The flame speed is much slower than that of the pressure wave and there is no interaction between the heat release and the pressure wave. In the latter, the spatial successive heat release constitutes a propagating combustion wave. If the propagation speed of this combustion wave is subsonic, there is again no heat release/ pressure wave interaction, since the heat release region is away from the pressure wave. Thus the combustion process is a deflagration for both cases, and acoustic knock results.

(c) Detonation

When R is sufficiently large to create a significant pressure ratio between the local pressure and the end gas pressure, the resulting shock wave could induce fast heat releasing chemical reactions in the end gas at the wave front (the normal Chapman-Jouguet denotation) [19]. Alternatively, the successive ignition along a gradient may be rapid enough to create a combustion wave with speed comparable to the local pressure wave propagation (sonic) speed. Then there is significant interaction between the heat release reaction and the pressure wave. The latter phenomenon has been termed developing detonation [13 18]. In both cases, the local post-combustion pressure is higher than the isochoric value at the end gas condition because of compression by the pressure wave.

The name "developing" detonation is confusing. If we broaden the definition of detonation from a combustion wave which is induced by the pressure wave to that which has significant interaction with the pressure wave, then both the normal and the developing detonation can be described by the term detonation since in both cases, the combustion wave and the pressure wave travel together, and there is significant interaction between them.

These detonation waves have been observed through high speed movies [11, 12, 20]. Detonation are very damaging to the combustion chambers; for example, the destruction of the piston top land is due to the detonation of the crevice gas by the shock wave propagating into the top land crevice [21].

In the remaining of the paper, the focus will be on (b), the acoustic knock mode of knock combustion. This mode is the most commonly encountered one in engine calibration because the flame initiation mode is usually not of concern (except for pre-ignition) and the detonation mode is so damaging that it is usually avoided.

Experimental

Knock combustion was studied using a modern production 2L, 4-cylinder, turbo-charged direct injection engine (GM LNF). The engine specification is shown in Table 1. The engine was controlled by an experimental ECU so that the valve and injection timings were set to the factory calibration values, but the spark timing and λ could be set by the operator. The original engine was not equipped with EGR; a low-pressure EGR loop was added. To avoid disrupting the turbocharger operation, the exhaust was not throttled so that the highest EGR level was limited to 12.5%.

The fuel used was Halterman HF437 calibration gasoline with RON of 96.6, MON of 88.5, and sensitivity of 8.1.

Data were collected over an extensive matrix of operating conditions in speed, load, spark timing, λ, and EGR; see Table 2.

Table 1. Engine specification; the valve timings are function of speed and load. The tabulated values are for 1500 rpm and 14 bar GIMEP for reference.

Engine type	Turbocharged in-line 4
Displaced volume	2L
Bore/ Stroke	86mm/ 86 mm
Compression ratio	9.2
IVO (@1500 rpm, 14 bar GIMEP)	31° btdc gas exchange
IVC (@1500 rpm, 14 bar GIMEP)	19° abdc compression
EVO (@1500 rpm, 14 bar GIMEP)	18° bbdc expansion
EVC (@1500 rpm, 14 bar GIMEP)	22 atdc gas exchange

Table 2. Range of operating conditions

Speed	1200 – 2000 rpm
GIMEP	8 – 14 bar
Spark timing	Various; from light to heavy knock
λ	0.8 to 1.3
EGR	0 to 12.5%

The quantity of interest is the knock intensity (KI), defined as the amplitude of the oscillation as recorded by the pressure transducer [7, 12]. The value of KI is determined from the high-passed pressure trace; see Fig. 3. A subjective threshold is set up so that a specific engine cycle is knocking if the cycle KI > 1 bar. An operating point (load, speed, λ, and EGR) is in knock condition if more than 10% of all cycles are knocking. (It is recognized that the pressure signal is dependent on the relative location of the knock region and the pressure transducer. This issue will be discussed in a later section.)
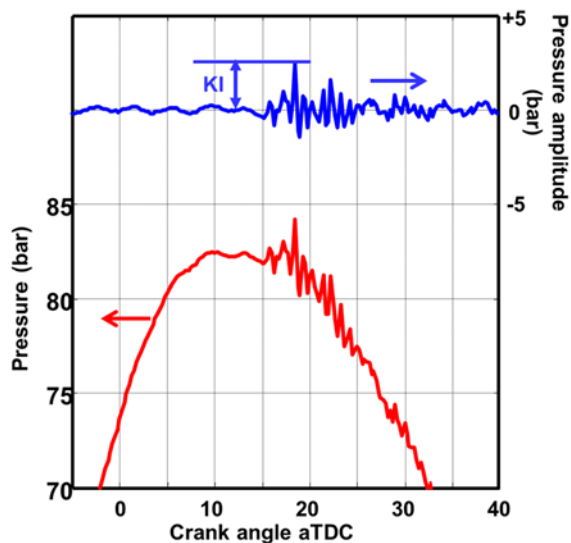

Figure 3. Determination of knock intensity.

KI statistics of acoustic knock

The matrix shown in Table 2 encompasses 336 run conditions covering the 5 variables; 99 consecutive cycles of knock data have been recorded for each condition (at 100 KHz sampling rate). Thus there are 336*99 = 33264 cycles of data. The KI values for each

cycle are plotted versus the GIMEP in Fig. 4. There is substantial scatter in the KI values at the same GIMEP. Both an increase of KI and the scatter of the KI values with GIMEP are observed.
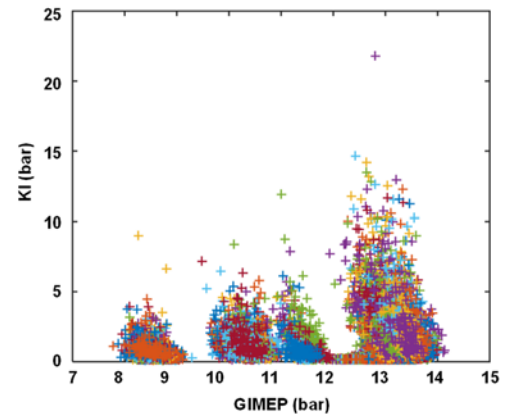

Figure 4. The KI values of individual cycles versus GIMEP; 33264 cycles of data encompassing 336 operating conditions with 99 consecutive cycles at each condition.

At a specific operating condition, there is also substantial scatter of the KI values; see Fig. 5 for a typical case. The KI appears to be random with no cycle-to-cycle correlation. Note that for the operating point shown (1250 rpm, 8.5 bar GIMEP, 0% EGR and λ =1), the mean value of KI is 1.6 bar, which is above the knocking threshold of 1 bar, and more than 10% of the cycles are knocking (with KI > 1 bar). Thus the operating point is consider as knocking. However, a significant number of the cycles (27 out of the 99) has KI< 1bar and thus are non-knocking cycles.
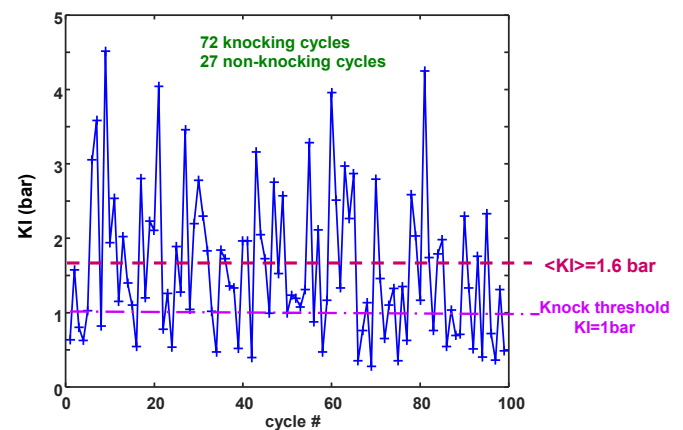

Figure 5. Knock intensity for 99 consecutive cycles; 1250 rpm, 8.5 bar GIMEP, λ = 1, no EGR.

From the above discussion, KI is clearly a random variable for which a statistical description is appropriate. The histogram of KI corresponding to the data shown in Fig. 5 is shown in Fig. 6. Because KI is definitely a positive quantity, a log normal distribution is fit to the data. The fit is also shown on the figure. The distribution is characterized by two parameters: μ (= mean of log(KI)), and σ (= standard deviation of log(KI)). So for an operating point, if the values of μ and σ are known, the KI distribution is determined. Thus the task is to relate μ and σ to the operating point parameters.
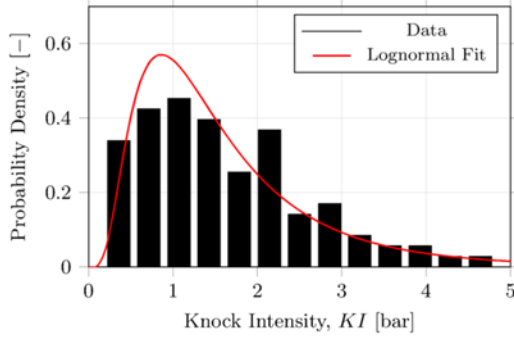
Figure 6. Probability distribution of knock intensity for 99 consecutive cycles; 1250 rpm, 8.5 bar GIMEP, λ = 1, no EGR.

Pressure build up in exothermic center

Because of charge non-uniformity, only finite regions (exothermic centers), usually of elevated temperature (but composition non-uniformity could also play a role), of the end gas auto-ignites. That KI does not correlate with the mass of the end gas [22] substantiates the above statement.

The size of the exothermic centers [23] depends on the extent of the charge non-uniformity. For illustration purpose, consider a one dimensional charge that is uniform in composition but with a temperature distribution T(x, t). Assume that auto-ignition is given by the Livengood-Wu integral

$$I(x,t) = \int_{t_{IVC}}^{t} \frac{dt'}{\tau(p(t'),T(x,t'))} \tag{4}$$

where τ is the ignition delay. Then at the time of ignition t*, the value I(x,t*) must reach 1 at some location. See dash line in Fig. 7.
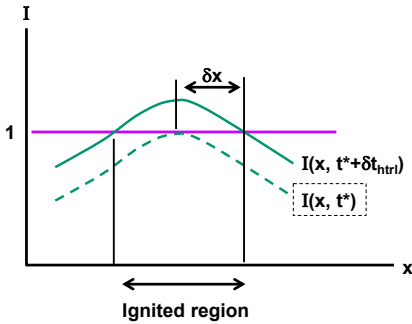

Figure 7. Schematic showing the determination of the ignited region.

If δt_{htrl} is the time for the heat releasing chemical reaction, the extent of the ignited region will be given by the width of the I(x,t) curve that crosses the I = 1 line at time $t + \delta t_{htrl}$; see Fig. 7.

The size of the ignited region, δx, is therefore:

$$\delta x = \delta t_{htrl} \left[\frac{\partial I / \partial t}{\partial I / \partial x} \right]_{t*} = \frac{1}{\tau*} \frac{\delta t_{htrl}}{[\partial I / \partial x]_{t*}} \tag{5}$$

where $\tau* = \tau(t*) = [(\partial I/\partial t)_{t*}]^{-1}$ is the ignition delay at the time of knock on set. Note that δx is proportional to $(\partial I/\partial t)$: how fast the I curve is rising in time. It is inversely proportional to the slope $(\partial I/\partial x)$

7/20/2015

of the I curve; thus for a large slope (a pointy I distribution), the ignition region will be small and will not excite pressure wave. This observation is consistent with the findings from numerical simulations [13].

The pressure build up δp in the exothermic center may be obtained by integrating Eq. (1) over the heat release time δt_{htrl}:

$$\delta p = (\gamma - 1)q - \gamma p \frac{\dot{V}}{V} \delta t_{htrl} \tag{6}$$

Note that q, the heat release per unit volume of the charge, is independent of the size of the ignition region. Thus the dependence of δp on δx comes from the pressure relief term (see Fig. 8). Typical values are given in Table 3. Typical heat release time is of the order of μs to tens of μs. Therefore exothermic centers of mm sizes would not excite pressure waves, but those of cm sizes would.
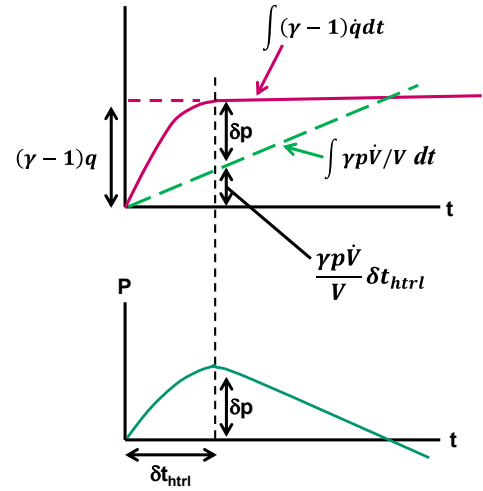

Figure 8. Pressure development of exothermic center.

Table 3. Contributions to the pressure rise in a spherical exothermic center; at p=30 bar; unburned temperature = 700K, λ =1.

Radius of spherical exothermic center	$(\gamma - 1)q$	$(\gamma - 1)p\left(\frac{\dot{V}}{V}\right)$
1 mm	140 bar	120 bar/μs
1 cm	140 bar	12 bar/μs

Correlations for μ and σ

Basis

Eq. (6) may be used as the basis for formulating a correlation for KI, which is proportional to δp. The volumetric heat release q scales with GIMEP. For the second term on the right hand side of Eq. (6), p scales with GIMEP/(1-EGR). The volumetric expansion term (for a spherical exothermic center) is:

$$\frac{\dot{V}}{V} \delta t_{htrl} = 3a \frac{\delta t_{htrel}}{\delta x} \tag{7}$$

Using Eq.(5) for δx, then

$$\frac{\dot{V}}{V}\delta t_{htrl} = 3a\tau *\left(\frac{\partial I}{\partial x}\right)_{t*} \tag{8}$$

Note that δt_{htrl} no longer appears in the expression; essentially, the effect of more time to relax the pressure cancels that of the larger exothermic center. The cancellation of δt_{htrl} is fortunate because its value is sensitive to the local temperature and pressure, which depend on the operating condition and cannot be modelled in a simple way.

The above discussion in relation to Eq.(6) suggests a correlation of the following:

$$\frac{KI}{GIMEP} = fn\left(C_1 - C_2\frac{\tau*}{(1-EGR)*GIMEP^\beta}\right) \tag{9}$$

Here, C_1 corresponds to $(\gamma -1)q/GIMEP$ and $C_2/(1-EGR)$ to γ $p/GIMEP$ when Eq. (6) is divided by GIMEP.

Note that the expression is not developed through vigorous logic: the term $(\partial I/\partial x)_{t*}$, which depends on the charge spatial non-uniformity, has been dropped because there is no easy way to account for its value. Likewise, the details of multiple exothermic center are not included. So the approach should be considered semi-empirical. The term $1/GIMEP^\beta$ has been added to account for any residual GIMEP dependence. The value of β is expected to be a small number.

Correlation development

The objective of the correlation development is to relate the parameters defining the statistical distribution of KI to the engine operating parameters. As such, except for KI, which varies from cycle-to-cycle, all quantities involved are the mean cycle properties. For a specific operating point, the individual cycle is indexed by j and cycle-averaging is denoted by $<>$; then:

$$GIMEP = <GIMEP_j> \qquad EGR = <EGR_j> \tag{10}$$

The time at knock point t* is solved from the Livengood-Wu integral with the cycle averaged properties $<p_j>$ and $<T_j>$:

$$1 = \int_{t_{IVC}}^{t*}\frac{dt'}{\tau(<p_j>,<T_j>)} \tag{11}$$

An established ignition delay correlation may be used for $\tau(p, T)$. The expression used here is the one developed using the data from the particular engine use in this experiment [24]. Then the ignition delay at knock point is

$$\tau* = \tau(p(t*),T(t*)) \tag{12}$$

For all the operating points, a log normal distribution is fit to the collection of $KI_j/GIMEP$ values so that

$$\mu = mean\left[\log_e(KI/GIMEP)\right]$$
$$\sigma = standard\ deviation\left[\log_e(KI/GIMEP)\right] \tag{13}$$

Then using the expression in Eq.(9), the correlation for μ is

$$\mu = 0.73 - \frac{5.02\tau*}{(1-EGR)\ GIMEP^{0.12}} \tag{14}$$

where GIMEP is in bar, and $\tau*$ is in ms. For the knocking cycles, the correlation for μ over the 336 operating conditions is shown in Fig. 9. The error bars are the 90% confidence brackets for the μ values in the log normal distribution fit to the data at the individual operating condition.

The correlation is quite satisfactory, considering the large number of operating conditions and the statistical nature of the data. That the correlation works implies that the dominant factor influencing KI is how fast the progression to ignition is (the $(\partial I/\partial t)_{t*}$ term in Eq.(5)).

On a closer examination (see the magnified plot in Fig. 9), there are data points which deviates from the fit. These points are largely at a different nominal GIMEP and the outlier data points line up with approximately the same slope as the main fit line. An explanation for this discrepancy is that the pressure signal recorded depends on the location of the pressure transducer relative to the exothermic center, which determines the spatial distribution of the acoustic mode. An extreme example is shown in Fig 10, which shows the pressure signals as recorded simultaneous by two transducers for the same knocking cycle. There is a large difference between the pressure signals because one of the transducers is at the spark plug location which is at the node of the pressure oscillation; hence it records a small pressure oscillation. There are however, optical data which show that the knock location tends to be at the same place [25]. So for a fixed pressure transducer location, the signal should be consistent. When the GIMEP changes, however, the knock location may change, and there would be a corresponding change in the transducer signal. The change in knock location may explain the deviations in the correlation.
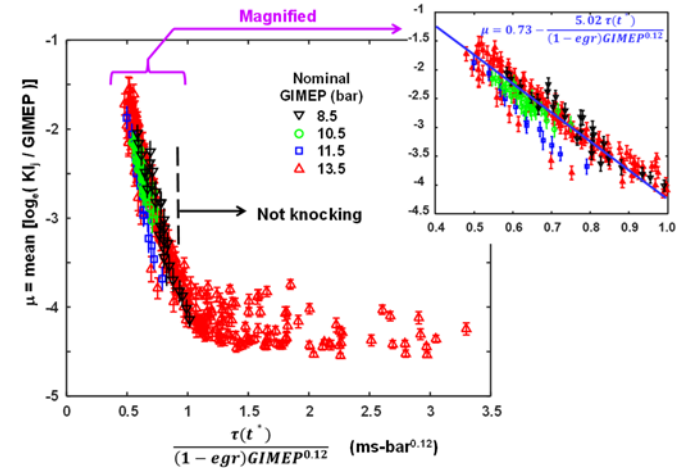

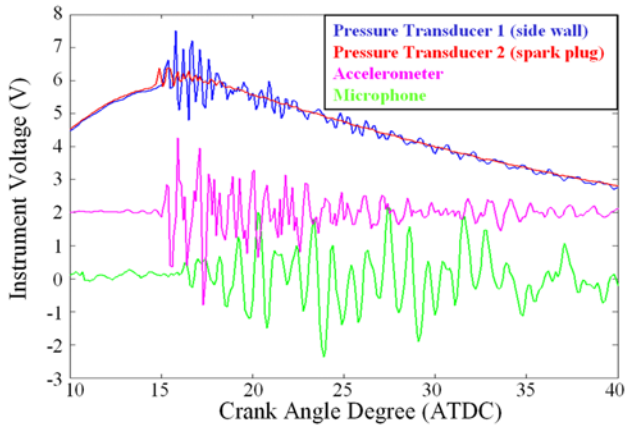Figure 9. Correlation for μ in terms of the mean cycle properties.

Figure 10. Pressure signals of a knocking cycle measured simultaneously by transducers mounted at two locations.

The standard deviation σ of log(KI/GIMEP) is shown in Fig. 11 against the correlation variable. The error bars represent the 90% confidence interval for σ in the fit of the log normal distribution to the data. Note that σ encompasses the effects of variations of combustion phasing, charge temperature and composition non-uniformity, and other factors. For the knocking cycles, it is remarkable that σ comes out to be approximately a constant:
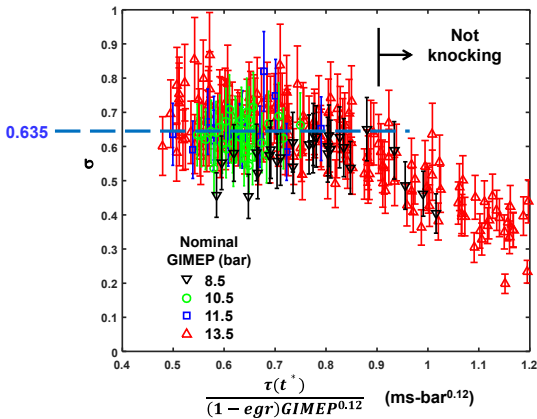
$$\sigma = 0.635 \tag{15}$$

Figure 11. Standard deviation of log(KI/GIMEP).

Utility

Although the above correlation is based on data from a single engine, the large set of operating conditions used in the development renders it a degree of robustness so that it is generally applicable to similar engines (approximately 500 cc per cylinder, turbo-charge with spray guided direct injection). The correlation can then be used to find the distribution of KI in an engine simulation at a given GIMEP as follows.

From the calculated pressure / temperature trajectory in the engine simulation, the knock point t* is determined using a correlation for the ignition delay τ. Then $\tau^* = \tau(t^*)$, hence μ can be found from Eq. (14). The value of σ is given in Eq. (15). The probability distribution function f of KI/GIMEP is log normal:

$$f\left(x \equiv \frac{KI}{GIMEP}; \mu, \sigma\right) = \frac{\exp\left\{\frac{-\left[\ln(x) - \mu\right]^2}{2\sigma^2}\right\}}{(x)\sigma\sqrt{2\pi}} \tag{16}$$

Thus if one sets a knock threshold at a knock intensity of KI*, the probability of knocking at the operating point being simulated is

$$\text{Probabiliy (KI>KI*)} = \int_{KI^*/GIMEP}^{\infty} f(x; \mu, \sigma)\,dx \tag{17}$$

As discussed in the last section, this calculation also does not take into account of the location of the pressure transducer relative to the spatial distribution of the acoustic oscillation. The knock intensity KI' recorded by the transducer, will be different from the "nominal" value KI by a factor of α. Then the probability distribution of KI' is the same log normal distribution but with a shift of μ; the σ value remains unchanged:

$$f\left(z \equiv \frac{KI'}{GIMEP}; \mu', \sigma\right) = \frac{\exp\left\{\frac{-\left[\ln(z) - (\mu')\right]^2}{2\sigma^2}\right\}}{z\sigma\sqrt{2\pi}} \tag{16}$$

$$\text{where} \qquad \mu' = \mu + \ln(\alpha)$$

Since engine simulations usually does not account for the pressure transducer location, the nominal value for μ (with $\alpha = 1$) would be a reasonable estimate.

Summary/Conclusions

Depending on the end gas non-uniformity, auto-ignition in a spark ignition engine could result in flame initiation, acoustic knock, or detonation (normal and developing). For acoustic knock, the knock intensity (KI), defined as the amplitude of the pressure oscillation, is statistical in nature. The value KI/GIMEP follows a log normal distribution with mean μ and standard deviation σ. Using data over a substantial range of operating points, a correlation of μ and σ to the engine operating condition is developed. The value of μ decreases linearly with the ignition delay at the knock point; σ is found to be a constant. This information could be used to determine the statistical distribution of KI in an engine simulation.

References

1. Heywood, J, *Internal Combustion Engine Fundamentals*, McGraw –Hill, ISBN 0-07-028637, 1988.
2. Fieweger, K., Blumenthal, R., and Adomeit, G., "Self-Ignition of SI Engine Model Fuels: A Shock Tube Investigation at High Pressure," *Comb. & Flame*, 109, pp599-619, 1997.
3. Minetti, R. Carlier, M., Ribaucour, M., Therssen, E., and Sochet, L.R., "A Rapid Compression Machine Investigation of Oxidation and Auto-Ignition of n-Heptane: Measurements and Modeling," *Comb. & Flame*, 102, 298-309, 1995.
4. Cox, R.A., Cole, J.A., "Chemical Aspects of the Autoignition of Hydrocarbon-Air Mixtures," *Comb. & Flame*, 60, 109-123, 1985.
5. Westbrook, C.K., Warnatz, J., and Pitz, W.J., "A Detailed Chemical Kinetic Reaction Mechanism for the Oxidation of iso-Octane and n-Heptane over an Extended Temperature Range

and its Applications to Analysis of Engine Knock," *22nd Symp. (Int.) on Combustion*, 893, The Combustion Institute, 1988.

6. Douaud, A., Eyzat, P., "Four-Octane-Number Method for Predicting the Anti-Knock Behavior of Fuels and Engines," SAE Paper 780080, 1980.

7. Hoepke, B., Jannsen, S., Kasseris, E., and Cheng, W.K., "EGR Effects on Boosted SI Engine Operation and Knock Integral Correlation," SAE Paper 2012-01-0707, 2012.

8. Kalghatgi, G., "Auto-Ignition Quality of Practical Fuels and Implications for Fuel Requirements of Future SI and HCCI Engines," SAE Paper 2005-01-0239, 2005.

9. Mittal, V., Heywood, J.B., "The Relevance of Fuel RON and MON to Knock Onset in Modern SI Engines," SAE Paper 2008-01-2414.

10. Livengood, J.C., Wu, P.C., "Correlation of Autoignition Phenomena in Internal Combustion Engines and Rapid Compression Machines," *5th Symp. (Int.) on Combustion*, 347-356, Reinhold Publ. Corp., 1955.

11. Male, T., "Photographs at 500,000 Frames Per Second for Combustion and Detonation in a Reciprocating Engine," *3rd Symp. (Int.) on Combustion, Flame and Explosion Phenomena*, 1949.

12. Spicher, U., Korger, H., and Ganser, J., "Detection of Knocking Combustion Using Simultaneously High Speed Schlieren Cinematography and Multi Optical Fiber Technique," SAE Paper 912312, 1991.

13. Konig, G, Maly, R.R., Bradley, D., Lau, A.K.C., and Sheppard, C.G.W., "Role of Exothermic Centres on Knock Initiation and Knock Damage," SAE Paper 902136, 1990.

14. Andreae, M., Cheng, W.K., Kenney, T., Yang, J., "On HCCI Engine Knock," SAE Paper 2007-01-1858, 2007.

15. Yelvington, P.E., Green, W.H., "Prediction of the Knock Limit and Viable Operating Range for a Homogeneous Charge Compression Ignition (HCCI) Engine," SAE Paper 2003-01-1092, 2003.

16. Zahdeh, A., Rothenberger, P., Nguyen, W., Anbarasu, M, et al, "Fundamental Approach to Investigate Pre-Ignition in Boosted SI Engines," SAE Paper 2011-01-0340, 2011.

17. Zeldovich, Y.B., "Regime Classification of an Exothermic Reaction with Nonuniform Initial Conditions," Comb. And Flame 39, 211-214, 1980.

18. Bradley,D., Morley, C., Gu, X.J., and Emerson, D.R., "Amplified Pressure Waves During Autoignition: Relevance to CAI Engines," SAE Paper 2002-01-2868, 2002.

19. Strehlow, R., *Combustion Fundamentals*, McGraw-Hill, 1984.

20. Qi, Y, Wang, Z., Wang, J., He, X, "Effects of Thermodynamic Conditions on the End Gas Combustion Mode Associated with Engine Knock," Comb. & Flame, 162, 11, pp 4119-4128, 2016.

21. Maly, R., Klein, R., Peters, N., Konig, G, "Theoretical and Experimental Investigation of Knock Induced Surface Destruction," SAE Paper 900025, 1990.

22. Konig, G., Sheppard, C.G.W., "End Gas Autoignition and Knock in a Spark Ignition Engine," SAE Paper 902135, 1990.

23. Oppenheim, A.K., "Dynamic Feaures of Combustion," Phil. Trans. R. Soc. London A, 315, 471-508, 1985.

24. McKenzie, J., Cheng, W.K., "Ignition Delay Correlation for Engine Operating with Lean and with Rich Fuel-Air Mixtures," paper submitted for 2015 SAE Congress (16PFL-0117).

25. Park, S., Furukawa, T., "Validation of Turbulent Combustion and Knocking Simulation in Spark-Ignition Engines Using Reduced Chemical Kinetics," SAE Paper 2015-01-0750, 2015.

Contact Information

Jacob McKenzie; jake.mkz@gmail.com
Wai Cheng; wkcheng@mit.edu

Acknowledgments

Definitions/Abbreviations

a	Velocity of sound
EGR	Mass fraction of exhaust gas recirculation in fresh charge.
GIMEP	Gross indicated mean effective pressure
I	Livengood-Wu integral
KI	Knock intensity
p	Pressure
q	Volumetric heat release
R	Radius of exothermic center (auto-ignited region)
t	Time
t*	Time at auto-ignition
T	Temperature
V	Volume
x	Coordinate
γ	Ratio of specific heats
δx	Size of exothermic center
δ_{htrl}	Time to burn out mixture in auto-ignited region
λ	Air fuel equivalence ratio
μ	Mean of log(KI/GIMEP)
σ	Standard deviation of log(KI/GIMEP)

7/20/2015